Scientific
Research
Publishing

Influence of Fine Zirconia Particle Shot Peening on Sliding Wear of Zirconia-Silicon Carbide Composites

Hitonobu Koike, Koji Takahashi

Yokohama National University, Yokohama, Japan
Email: koike-hitonobu-rp@ynu.jp, takahashi-koji-ph@ynu.ac.jp

Abstract

In this paper, the sliding contact fatigue wear performance of shot-peened zirconia-silicon carbide composite (ZrO_2/SiC) plates in contact with silicon nitride balls under compressive residual stress in dry conditions was investigated in order to improve the wear resistance of ZrO_2/SiC friction parts. The wear resistance of ZrO_2/SiC plates after shot peening was higher than that of plates not treated with shot peening in sliding wear testing under Hertzian-contact. Due to fine Zirconia particle shot peening, the tetragonal phase crystal structure in ZrO_2 in the near-surface of ZrO_2/SiC plates was changed, and 1100 MPa compressive residual stress could be introduced into the near-surface layer of ZrO_2/SiC plates. The compressive residual stress was determined to be the main factor in the improvement of the sliding wear resistance of ZrO_2/SiC plates.

1. Introduction

Zirconia (ZrO_2) composites have great potential as moving parts in special situations for machine elements or medical apparatus. They have low densities, high hardness, high temperature durability and biocompatibility [1] [2] [3]. Particularly the wear resistance is one of the most important properties for moving parts such as bearing or joints. Because severe wear at the contact areas in friction zones of moving parts affects the device's lifespan and stable movement. Recently the tribological behavior on ZrO_2 was studied by many researchers [4] [5] [6] in order to evaluate the quality problems such as failure of ceramic's part. Mechanical sliding wear of ceramics under dry conditions is a process of conti-

nuous micro-fracturing from many cracks, in fact, sliding wear related to fracture toughness. Hokkirigawa [7] proposed that the sliding wear of ceramics is related to both K_{eff} and P_{max} and crack length.

In order to improve the friction surface of ZrO_2 composites reinforced by silicon carbide (ZrO_2/SiC) for practical use, this study focused on shot peening (SP). SP is a well-known surface treatment technique for improving fatigue strength of metal parts. In a typical SP process, a stream of small, hard spheres is shot at a treated surface. After SP, compressive residual stress is generated underneath the treated surface, due to localized plastic deformation in the near-surface layer. Pfeiffer et al. [8] found that compressive residual stress could also be introduced into the near-surface of silicon nitride (Si_3N_4) using a novel SP method. As a result of SP effects, the resistance of the bearing raceway against surface fatigue damage (severe pitting and chipping) increased [8]. Takahashi et al. [9] [10] [11] [12], in addition, reported that the compressive residual stress occurred in the near-surface region of shot-peened partially-stabilized zirconia (PSZ) [9], Si_3N_4 [10] [11], or Al_2O_3 [12]. The compressive residual stresses at the PSZ and Si_3N_4 surfaces after SP were approximately 1400 MPa and 880 MPa, respectively. The compressive residual stresses significantly increased PSZ's fracture toughness and bending strength [9]. Koike et al. [13] stated the wear durability of PSZ after SP was better than that of PSZ without SP. However, the mechanism behind this increase in wear durability of ZrO_2/SiC composites under compressive residual stress by SP stress was not clear.

Some researchers have reported phase transformation or domain switching as a result of the application of tensile or compressive stress. Tetragonal-to-monoclinic phase transformation [14] [15] and ferroelastic domain switching [16] [17] are well-known mechanisms for toughening of ZrO_2. Mc Meeking et al. [15] presented that tetragonal-to-monoclinic phase transformation, for one, prevents crack propagation at the crack tip because of the crack closure effect. Kiguchi et al. [16] and Virkar et al. [17] reported the second mechanism as reorientation of ferroelastic domains by externally applied stress. Kiguchi et al. [16] stated that the application of compressive stress converted the c axis into an a axis in lattice constants in the tetragonal phase of ZrO_2.

As mentioned, the wear properties of shot-peened PSZ were investigated previously [13]. However, the effects of SP on the wear resistance of ZrO_2/SiC composites have not been investigated yet. In addition, microstructural changes after SP, such as domain switching, are unclear. In this work, therefore, the sliding wear properties of the shot-peened ZrO_2 reinforced by silicon carbide (ZrO_2/SiC) were examined under dry conditions. The near-surface of the ZrO_2/SiC plates was examined by X-ray measurements in order to explore their microstructural changes after SP.

2. Materials and Methods

2.1. Materials and Shot Peening Procedure

ZrO_2 reinforced by silicon carbide (ZrO_2/SiC) was selected as the test material.

Wear test specimens were fabricated from ZrO_2 powder containing 3 mol%Y_2O_3 and 20 vol% SiC powders. After mixing of ZrO_2/SiC with ethanol by ball milling for 24 h, the powder was dried in a vacuum chamber. The dry powder was hot-pressed under vacuum at 1450°C and 30 MPa for 1 h. The hot-pressed materials were cut into plates. The size of the ZrO_2/SiC plates was 25 mm × 25 mm × 4 mm (length × width × thickness). The density of this material was 6.05 g/cm³. ZrO_2/SiC plate specimens with and without SP are referred to as SP and Non-SP specimens. For SP, ZrO_2 beads with a diameter of 180 μm, air pressure of 0.2 MPa, and peening time of 20 s were used. SP coverage was approximately 200%, meaning that the complete ZrO_2/SiC plate surface was shot-peened twice. The brittle ZrO_2/SiC were not cracked by the shots when the air pressure was lower than 0.2 MPa. It was suitable condition for compressive residual stress by SP. Finally, after SP, ZrO_2/SiC plate surfaces were polished with a 0.1 μm diameter diamond solution to truncate the edges on dimples caused by SP. The surface roughness of all samples was measured using a profilometer, with three repeated measurements per sample. The Vickers hardness (HV) of Non-SP and SP plates was measured by a hardness tester using a load of 98 N and indentation time of 20 s.

2.2. Sliding Contact Wear Test Setup

Figure 1 illustrates the ball-on-plate sliding wear test at room temperature. Si_3N_4 balls (grade 3) with 4.76 mm diameter and Vickers hardness of 1600 HV were used as wear counterparts. Sliding wear tests were performed by using a friction wear test machine in reciprocation mode, with a reciprocation length of 10 mm. The vertical loads Q ranged from 2.94 to 9.80 N, corresponding to a mean Hertzian contact pressure (P_{mean}) ranging between 816 and 1219 MPa. The maximum Hertzian contact pressures P_{max} ranged between 1220 and 1830 MPa. Values for P_{mean} and P_{max} were calculated from the following equations [18].

$$a = \sqrt[3]{\frac{3RQ}{4}\left\{\frac{\left(1-v_1^2\right)}{E_1}+\frac{\left(1-v_2^2\right)}{E_2}\right\}} \tag{1}$$

$$P_{\text{mean}} = \frac{Q}{\pi a^2}, P_{\text{max}} = 1.5 P_{\text{mean}} \tag{2}$$

In the above, v_1 and v_2 are the Poisson's ratios for ball and plate materials, respectively; $v_1 = 0.28$ and $v_2 = 0.28$. E_1 and E_2 are the Young's moduli for ball and plate materials, respectively; $E_1 = 300$ GPa and $E_2 = 214$ GPa. Q [N] is the vertical load, a [m] is the contact area radius, and R is the ball radius. The sliding velocity and frequency were 0.033 m/s and 1.7 Hz, which corresponds to 100 reciprocation cycles per minute. The total wear path length and total duration were 800 m and 400 min, respectively. In order to calculate the wear volume (W_{vol}) of ZrO_2/SiC plates after the test, the wear depth (W_{dep}) and width (W_{wid}) were measured at three different areas of each specimen using a profilometer. Equation (3) was used to calculate W_{vol}.

$$W_{\text{vol}} = 0.5 \times W_{\text{dep}} \times W_{\text{wid}} \times 10 \tag{3}$$
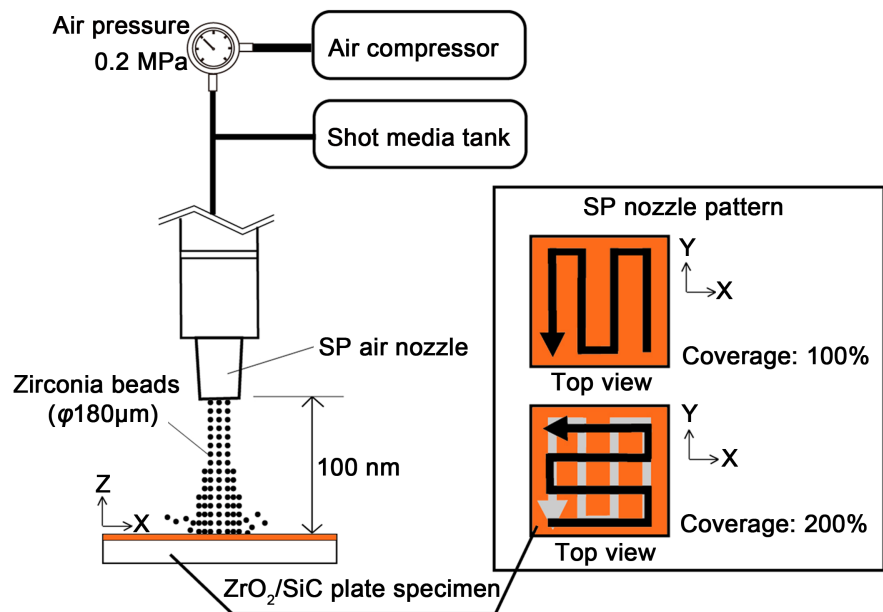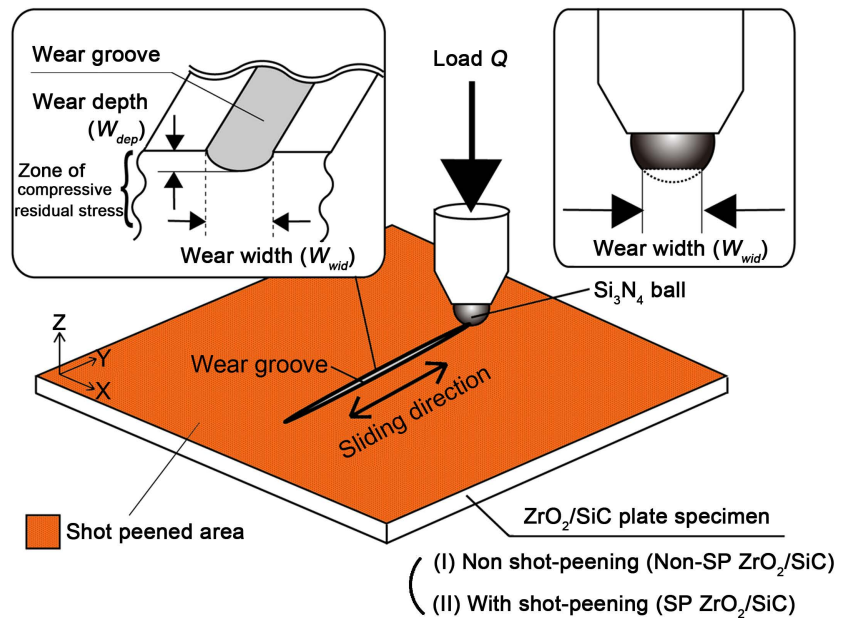
Figure 1. Schematic illustration of the sliding wear test in reciprocation mode, and shot peening pattern.

In the above, the cross-sectional area of the wear groove was approximated as a triangular area ($=0.5 \times W_{dep} \times W_{wid}$), which was multiplied by the reciprocation length (10 mm). The ball and plate specimens prior to and after the tests were observed using an optical microscope with polarized light.

2.3. XRD Measurements

To evaluate residual stress and crystal structures at the near-surface of ZrO_2/SiC plates, XRD measurements were taken. Table 1 lists the conditions for measurement of residual stress, which was estimated using the 2θ-$\sin^2 \Psi$ method.

Table 1. Conditions of residual stress measurements.

X-ray diffraction (XRD) equipment	Ultima IV (Rigaku corp.)
Characteristic X-ray	CrKα (For residual stress of (1 3 3) plane)
Diffraction plane	tetragonal (1 3 3)
Diffraction angle (deg)	153.50
X-ray stress constant (MPa/deg)	−283 [19]
Tube voltage (kV)	40
Tube current (mA)	40

The CrKα wavelength was 2.29Å. Tanaka *et al.* [19] stated the penetration depth of CrKα radiation was estimated as 2 - 3 μm.

3. Experimental Results and Discussion

3.1. Surface Observation after Shot-Peening

Figure 2 shows optical microscope and scanning probe microscope (SPM) images of Non-SP and SP plates. Submicron-sized dimples were formed on the surface of the SP ZrO_2/SiC plates by the impact of the ZrO_2 beads. Table 2 shows the average roughness (R_a) and maximum roughness height (R_z) of Non-SP and SP plates. The R_a values of the SP plates after polishing and the Non-SP plates were identical. The R_z of the SP plate after polishing was0.73 μm, slightly higher than that of the Non-SP plate (R_z = 0.57 μm), due to the fact that the submicron-sized dimples induced by SP were not completely removed by polishing.

3.2. Hardness

The HV of Non-SP and SP ZrO_2/SiC plates was 1260 HV and 1398 HV, respectively, similar to the HV of Non-SP PSZ and SP ZrO_2 plates (1293 HV and 1328 HV, respectively) [13]. SP thus caused an increase in HV of both materials [9] [13]. It was thought that the hardness of both materials increased because strain hardening or recrystallization occurred due to SP. Figure 3 shows microscopic images of Vickers indentations on the surfaces of Non-SP and SP ZrO_2/SiC plates. The apparent fracture toughness of the Non-SPZrO_2/SiC plate was calculated 8.9 MPa·m$^{0.5}$ by Indentation Fracture method. However, no radial cracks were formed on the SP ZrO_2/SiC plates due to the effects of compressive residual stress, indicating that the apparent fracture toughness of ZrO_2/SiC plates was improved by SP.

3.3. Sliding Wear Test

Figure 4(a) shows optical microscope image of friction surface on the raceway of shot-peened ZrO_2/SiC plate after the wear test at P_{mean} = 967 MPa. Microplowings can be observed on both the SP and Non-SP plates. These microplowings were caused by traction of wear particles. Abrasive wear was main wear mechanism in the tests. Adhesive wear was rarely observed. Figure 4(b) shows the optical microscope image of friction surface on the Si_3N_4 balls after wear
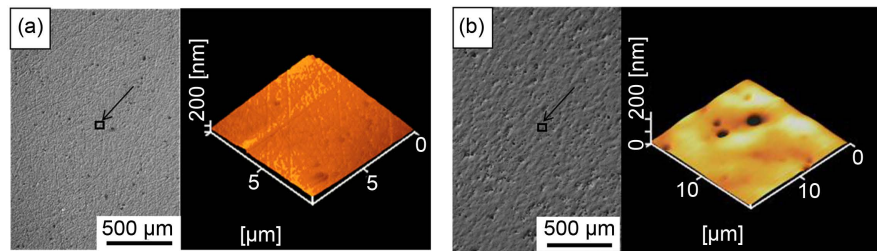
Figure 2. Optical microscope (left) and surface topography (right) prior to the test: (a) Non-SP, (b) SP.
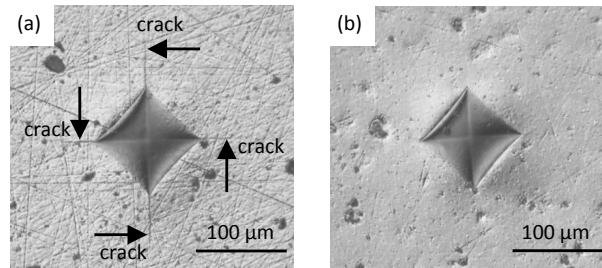
Figure 3. Vickers indentation and radial cracks; (a) Non-SP plate, (b) SP plate.
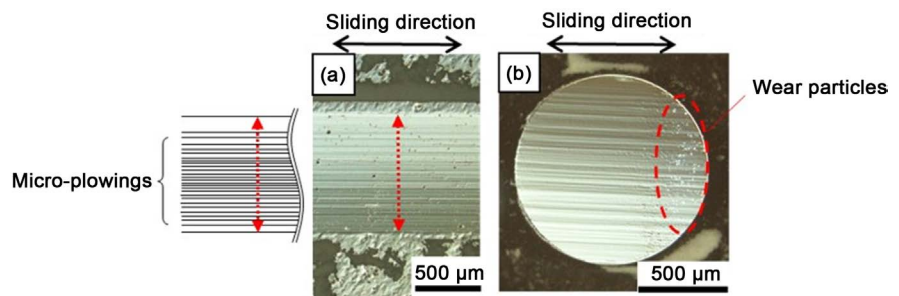
Figure 4. Optical micrographs of the friction surfaces; (a) raceway of the shot-peened ZrO_2/SiC plate and (b) the Si_3N_4 ball after 8×10^4 cycles at $P_{mean} = 967$ MPa. Note that the dot-lined arrows indicate the W_{wid}.

Table 2. Surface roughness of Non-shot-peened (Non-SP) and shot-peened (SP) plates.

	Non-SP	SP
Average roughness, R_a (μm)	0.04	0.04
Maximum height roughness, R_z (μm)	0.57	0.73

testing. Micro-plowings and wear particles can be observed, similar as on the ZrO_2/SiC plates. Powder-like wear particles accumulated on the sliding area near the edge of the balls. These wear particles caused micro- plowings along sliding tracks on the friction surfaces of both balls and plates.

Figure 5 shows the W_{vol} values of ZrO_2/SiC plates after 8×10^4 cycles. The W_{vol} of the SP ZrO_2/SiC plates clearly smaller than that of Non-SP plates. Figure 6 shows the W_{wid} of the Si_3N_4 balls after 8×10^4 cycles. The W_{wid} values of the Si_3N_4 balls used for tests on the SP plates were lower than those of balls used for tests on Non-SP plates. The aggressiveness to Si_3N_4 balls was also reduced when
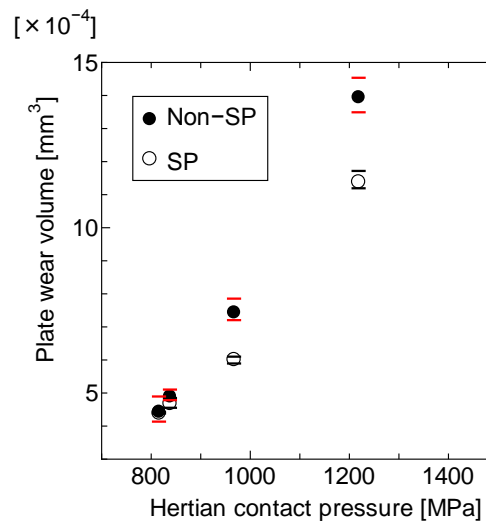
Figure 5. Comparison of plate wear volume for SP and Non-SP ZrO_2/SiC plates after 8×10^4 cycles.
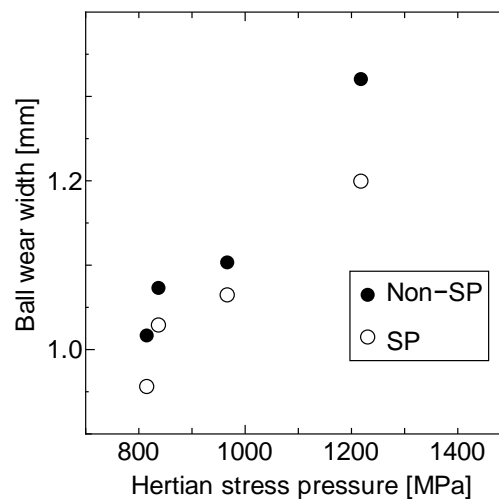
Figure 6. Comparison of wear width (W_{wid}) of Si_3N_4 ball tested against SP and Non-SP ZrO_2/SiC plates after 8×10^4 cycles.

the shot-peened ZrO_2/SiC plates were polished. Thus, SP increased the sliding fatigue wear resistance of the ZrO_2/SiC plates and the Si_3N_4 balls.

Figure 7 shows the friction coefficients of the SP and Non-SP plates during wear testing at P_{mean} = 967 MPa. Each diamond symbol represents the average value of the friction coefficient during 2×10^4 reciprocation cycles. The average frictional coefficients of SP and Non-SP plates were almost identical at 0.65 and 0.63, respectively. Thus, the submicron-sized dimples on the surface of SP ZrO_2/SiC plates shown in **Figure 2(b)** had little influence on the friction performance.

3.4. XRD Measurements

The measured value of compressive residual stress on the surface of SP ZrO_2/SiC plates was approximately 1100 MPa as shown in **Figure 8**. The compressive residual stress of ZrO_2/SiC was higher than that of Si_3N_4/SiC or Al_2O_3/SiC. The
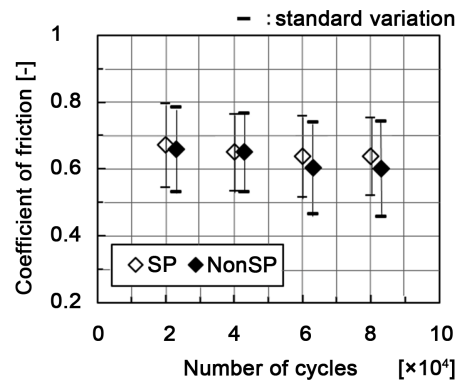
Figure 7. Friction coefficients of Non-SP and SP ZrO_2/SiC plates in contact with an Si_3N_4 ball at P_{mean} = 967 MPa.
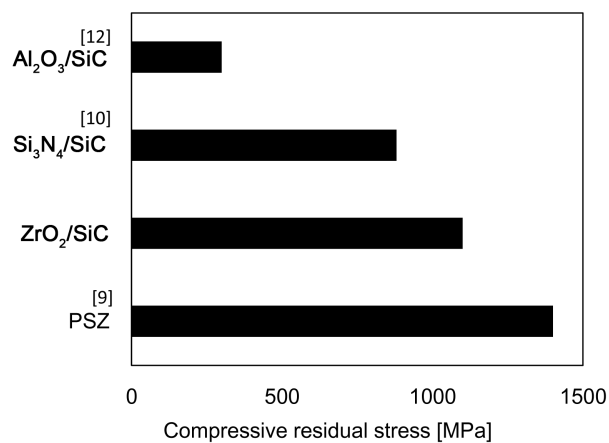
Figure 8. Compressive residual stress of the ZrO_2/SiC plate surfaces.

compressive residual stress on the surface of PSZ was 1400 MPa [9]. Thus, the compressive residual stress of ZrO_2/SiC was lower than that of PSZ, even though the SP conditions were almost the same. It is thought that the SiC particles between the grain boundaries of ZrO_2 locally restrained plastic deformation of ZrO_2.

Figure 9 show the XRD profiles in the near-surface regions of ZrO_2/SiC plates. The monoclinic (-111) peak after SP was only slightly detected. This means that tetragonal-to-monoclinic phase transformation was not main reason of large compressive stress on the ZrO_2/SiC plate surfaces in the SP condition. However, The peaks around 2θ = 35˚, corresponding to tetragonal phases in ZrO_2 crystal structure, changed after SP [20]. The relative integrated intensities of the tetragonal (002) peak and the tetragonal (200) peak changed after SP, as shown in **Figure 9**. The peak intensity ratios (X) for Non-SP and SP specimens were calculated according to Equation (4).

$$X = \frac{I_t(002)}{I_t(200)} \tag{4}$$

In the above, I_t(002) and I_t(200) are peak intensities of the tetragonal (002) at 2θ = 34.7˚ and (200) at 2θ = 35.2˚, respectively. The X for Non-SP and SP plates
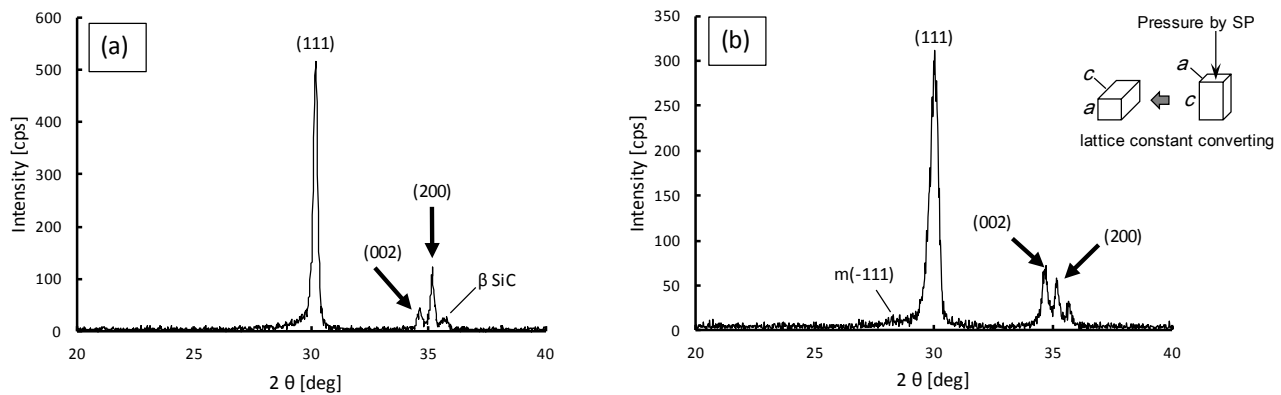
Figure 9. XRD measurements of the ZrO$_2$/SiC plate surfaces; (a) Non-SP, (b) SP. Note that arrows are reference points.

was 0.303 and 1.412, respectively. The X for the SP plates was therefore 466% higher than that for Non-SP plates. Thus, the lattice constants of tetragonal phase in ZrO$_2$ were changed due to SP. This means that the lattice strain in the tetragonal phase in ZrO$_2$ increased after SP, which is one of the reasons that large compressive residual stress could be introduced into the near-surface of the ZrO$_2$ specimens. This phenomenon was considered to be the switching of lattice constants (a and c in **Figure 10**) due to compressive contact stress during SP, likely causing toughening in ZrO$_2$ due to ferroelastic domain switching [16]. Upon compressive residual stress generation in ZrO$_2$, several mechanisms are proposed to take place; plastic deformation, phase transformation or domain switching. In ZrO$_2$/SiC plates under SP conditions, it is thought that domain switching was one of the main mechanism of residual stress generation. Virkar *et al.* stated that the application of compressive stress exceeding 1650 MPa along the c axis converts the c axis to an a axis, while one of the a axes converts to a c axis [17]. Tanaka *et al.* [19] and Scott [21] reported that the lattice constants in tetragonal crystalline PSZ were a = 0.510 nm and c = 0.519 nm, respectively. In fact, due to contact stress of SP, the c axis in the tetragonal phase converts to an a axis, and correspondingly the a axis stretched into a c axis. As the c axis of the tetragonal phase in ZrO$_2$ was shortened by 0.009 nm along the compressive direction, the lattice constant changed: the (200) c axis was converted to (002) as shown in **Figure 9**. Thus ferroelastic domain switching as the lattice constant change in the tetragonal phase in ZrO$_2$ affects the large compressive residual stress generation.

3.5. Sliding Wear of ZrO$_2$/SiC under Compressive Residual Stress

Figure 11 illustrates the wear particle contact abrasion model. Micro-plowing occurred due to wear particle indentation and abrasion between the Si$_3$N$_4$ balls and the ZrO$_2$/SiC plates. The wear particles were formed by fractures from micro-sized radial cracks, micro-flaking, or micro-pitting in the near-surface of the plates. Continuous micro-flaking affects the increasing amount of wear of the ZrO$_2$/SiC plate. When compressive residual stress is introduced into the near-surface of the SP ZrO$_2$/SiC plates, radial cracks can be closed. Cracks are,
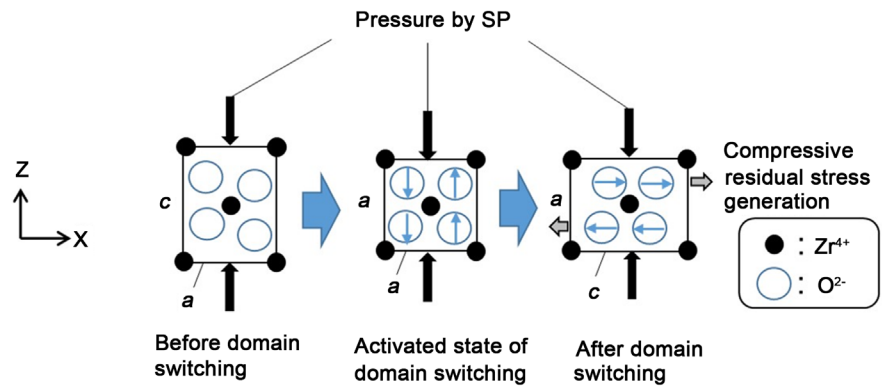
Figure 10. Schematic diagram of ferroelastic domain switching by SP. Note that the domain switching theory is cited from reference [16].
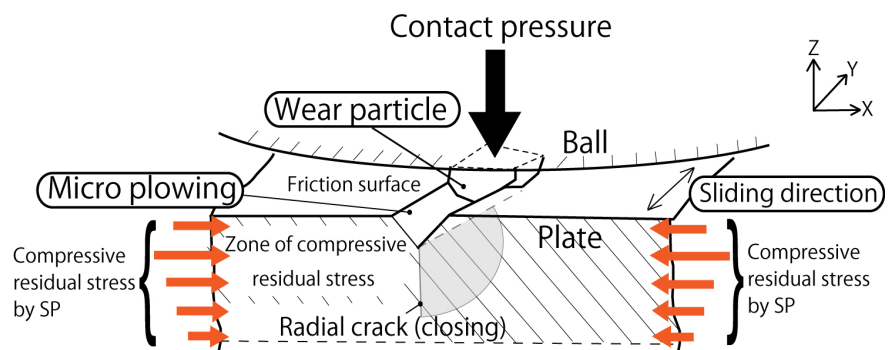
Figure 11. Improvement mechanism of sliding fatigue wear of the ZrO$_2$/SiC plates under compressive residual stress. Note that radial cracks could be closed by compressive residual stress.

thus, arrested by the closure effect due to compressive residual stress, which is the mechanism behind the improvement of wear resistance in SP ZrO$_2$/SiC composite ceramics. Additionally, the large compressive residual stress related to plastic deformation and ferroelastic domain switching affects wear resistance on the ZrO$_2$/SiC plate. As noted in 3.2. Hardness section, the apparent fracture toughness and hardness increased due to SP. These properties are also related to compressive residual stress, and improve the wear resistance at the ZrO$_2$/SiC plate surface. From the above results and discussion, it can be concluded that SP increased the wear resistance of ZrO$_2$/SiC plates against Si$_3$N$_4$ ball in the sliding wear test by increasing the compressive residual stress.

4. Conclusions

In order to improve the sliding fatigue wear resistance of Zirconia-Silicon Carbide Composites (ZrO$_2$/SiC) for frictional parts, the surface of ZrO$_2$/SiC plates was strengthened by shot peening (SP). Shot-peened plates were evaluated through sliding wear tests using a mean Hertzian contact pressure ranging from 816 to 1219 MPa, and the compressive residual stress and profile were examined using X-ray diffraction. From the obtained experimental results, the following conclusions were drawn:

1) The sliding fatigue wear resistance of shot-peened ZrO_2/SiC plates against Si_3N_4 balls was better than that of Non-SP plates. The aggressiveness to Si_3N_4 balls was also reduced when the shot-peened ZrO_2/SiC plates were polished.

2) SP could introduce a compressive residual stress of approximately 1100 MPa in the near-surface of ZrO_2/SiC plates. This compressive residual stress improved the sliding fatigue wear resistance against radial cracks. In addition, the surface hardness of ZrO_2/SiC plates also increased.

3) Due to SP, the XRD profile in the near-surface of the ZrO_2/SiC plates changed; the lattice constants in the tetragonal phase shortened in the compressive direction. Domain switching was one of the main mechanisms of large compressive residual stress generation in the near-surface of the plates. This microstructural change effectively closes radial cracks in the ZrO_2/SiC plates, which improve the sliding fatigue wear resistance of ZrO_2/SiC plates.

Acknowledgements

References

[1] Harrer, W., Deluca, M. and Morrell, R. (2014) Failure Analysis of a Ceramic Ball Race Bearing Made of Y-TZP Zirconia. *Engineering Failure Analysis*, **36**, 262-268.

[2] Preis, V., Behr, M., Handel, G., Schneider-Feyrer, S., Hahnel, S. and Rosentritt, M. (2012) Wear Performance of Dental Ceramics after Grinding and Polishing Treatments. *Journal of the Mechanical Behavior of Biomedical Materials*, **10**, 13-22.

[3] Aboushelib, M.N. (2010) Long Term Fatigue Behavior of Zirconia Based Dental Ceramics. *Materials*, **3**, 2975-2985. https://doi.org/10.3390/ma3052975

[4] Kato, K. (2000) Wear in Relation to Friction—A Review. *Wear*, **241**, 151-157.

[5] Adachi, K., Kato, K. and Chen, N. (1997) Wear Map of Ceramics. *Wear*, **203-204**, 291-301.

[6] Kato, K. and Adachi, K. (2002) Wear of Advance Ceramics. *Wear*, **253**, 1097-1104.

[7] Hokkirigawa, K. (1991) Wear Mode Map of Ceramics. *Wear*, **151**, 219-228.

[8] Pfeiffer, W. and Frey, T. (2006) Strengthening of Ceramics by Shot Peening. *Journal of the European Ceramic Society*, **26**, 2639-2645.

[9] Takahashi, K., Iwanaka, K., Osada, T. and Koike, H. (2015) Increase in Strength of Partially Stabilized Zirconia after Shot Peening. *Journal of Materials Engineering and Performance*, **24**, 9, 3573-3578. https://doi.org/10.1007/s11665-015-1623-x

[10] Takahashi, K., Nishio, Y., Kimura, Y. and Ando, K. (2010) Improvement of Strength and Reliability of Ceramics by Shot Peening and Crack Healing. *Journal of the European Ceramic Society*, **30**, 3047-3052.

[11] Takahashi, K. and Nishio, Y. (2012) Improvement of the Contact Strength of Si_3N_4/SiC by a Comparison of Shot Peening and Crack-Healing. *Journal of Solid Mechanics and Materials Engineering*, **6**, 144-153. https://doi.org/10.1299/jmmp.6.144

[12] Oki, T., Yamamoto, H., Osada, T. and Takahashi, K. (2013) Improvement of the Contact Strength of Al2O3/SiC bya Combination of Shot Peening and Crack-Healing. *Journal of Powder Technology*, **2013**, Article ID: 946984. https://doi.org/10.1155/2013/946984

[13] Koike, H., Iwanaka, K. and Takahashi, K. (2014) Measurement of Sliding Wear of Shot-Peened Partially Stabilized Zirconia Plate. *Applied Mechanics and Materials*, **597**, 353-357. https://doi.org/10.4028/www.scientific.net/AMM.597.353

[14] Guazzato, M., Albakry, M., Ringer, S.P. and Swain, M.V. (2004) Strength, Fracture Toughness and Microstructure of a Selection of All-Ceramic Materials. Part II. Zirconia-Based Dental Ceramics. *Dental Materials*, **20**, 5, 449-56.

[15] McMeeking, R.M. and Evans, A.G. (1982) Mechanics of Transformation-Toughening in Brittle Materials. *Journal of the American Ceramic Society*, **65**, 242. https://doi.org/10.1111/j.1151-2916.1982.tb10426.x

[16] Kiguchi, T., Urushihara, W., Saiki, A., Shinozaki, K. and Mizutani, N. (1996) Effect of Stress and Temperature on Ferroelastic Domain Switching of Partially Stabilized Zirconia Pseudo-Single Crystals. *Journal of the Ceramic Society of Japan*, **104**, 529-534. (In Japanese) https://doi.org/10.2109/jcersj.104.529

[17] Virkar, A.V. and Matsumoto, R.L.K. (1986) Ferroelastic Domain Switching as a Toughening Mechanism in Tetragonal Zirconia. *Journal of the American Ceramic Society*, **69**, C224-C226. https://doi.org/10.1111/j.1151-2916.1986.tb07341.x

[18] Hertz, H. (1881) Über die Berührung fester elastischerKörper. *Journal Für die Reine und Angewandte Mathematik*, **92**, 156-171. http://eudml.org/doc/148490

[19] Tanaka, K., Kurimura, T., Akiniwa, Y., Suzuki, K. and Nakagawa, H. (1989) X-Ray Residual Stress Measurement of Yttria-Partially Stabilized Zirconia. *Transactions of the Japan Society of Mechanical Engineers*, **55**, 318-325. (In Japanese) https://doi.org/10.1299/kikaia.55.318

[20] Houjou, K. and Takahashi, K. (2012) Crack-Healing Behavior of ZrO_2/SiC Composite Ceramics and Strength Properties of Crack-Healing Specimens. *International Journal of Structural Integrity*, **3**, 41-52. https://doi.org/10.1108/17579861211209984

[21] Scott, H.G. (1975) Phase Relationships in the Zirconia-Yttria System. *Journal of Material Science*, **10**, 1527-1535. https://doi.org/10.1007/BF01031853